^{13}C NMR study of the metal-insulator transition in $(DMe\text{-}DCNQI)_2Cu$ systems with partial deuteration

A. Kawamoto
Department of Physics, Faculty of Science, Ochanomizu University, Bunkyo-ku, Tokyo 112, Japan

K. Miyagawa
Department of Applied Physics, University of Tokyo, Hongo, Bunkyo-ku, Tokyo 113, Japan

K. Kanoda
Department of Applied Physics, University of Tokyo, Hongo, Bunkyo-ku, Tokyo 113, Japan
and Institute for Molecular Science, Myodaiji, Okazaki 444, Japan
(Received 31 December 1997)

The electronic states of a series of $(DMe\text{-}DCNQI)_2Cu$ systems with nondeuterated and partially deuterated methyl groups in a DMe-DCNQI molecule have been investigated by ^{13}C NMR measurements at the cyano carbon sites. The Knight shift of the nondeuterated specimen, which is metallic in the whole temperature range, is not scaled to the total spin susceptibility, demonstrating that the metallic state has several electronic bands with different local spin susceptibility due to the π-d hybridization. In the insulating phases of the partially deuterated specimens, ^{13}C NMR spectra are split into two lines, one of which has a nearly zero shift and the other has a large positive shift with the Curie-Weiss temperature dependence. The former line comes from the cyano group coordinated to the nonmagnetic Cu^+ ion, while the latter comes from the cyano group coordinated to the magnetic Cu^{2+} ion. The sign of the shift and intensity analysis provide an evidence that, in the insulating phase, spin is localized exclusively at one-third of the Cu sites without any population on the DCNQI molecule. This is considered as a manifestation of strong electron correlation in the Cu sites. The low-temperature reentrant metallic state in the partially deuterated system is found to be just the same as the stable metallic state in the nondeuterated system through the shift and relaxation rate behaviors. No fluctuations are observed in the vicinity of the metal-insulator and insulator-metal reentrant transitions, showing that the transitions are of the first order. [S0163-1829(98)01628-2]

I. INTRODUCTION

The $(R_1,R_2\text{-DCNQI})_2Cu$ (where $R_1,R_2=CH_3$, CH_3O, Cl, Br, I, etc.) systems have given frontiers for the study of the charge-transfer complexes containing organic molecules and metallic ions.[1] The R_1,R_2-DCNQI molecules make uniform one-dimensional columns along the c axis and the Cu ions are coordinated to the N atoms in the R_1,R_2-DCNQI molecules.[2] These salts are interesting with respect to the so-called π-d interaction between the one-dimensional conducting π band of the R_1,R_2-DCNQI molecules and the d orbitals of the Cu counter ions. The $(R_1,R_2\text{-DCNQI})_2Cu$ family shows a variety of conducting behaviors such as the metallic state in the whole temperature range (group I), the metal-insulator transition with an antiferromagnetic ordering at a low temperature (group II), and the reentrant (metal-insulator-metal) transition (group III).[3] While $(DMe\text{-}DCNQI)_2Cu$ ($R_1,R_2,=CH_3$) belongs to the group I at ambient pressure, this salt comes to show the group III or group II property by applying pressure.[4,5] The pressure-temperature phase diagram for the system with R_1,R_2, $=CH_3$ is depicted in Fig. 1.[6] It is widely accepted that the partial deuteration of DMe-DCNQI molecules is equivalent to the fine tuning of pressure.[7] The control of this ''chemical pressure'' can be made by alloying the nondeuterated and fully deuterated DMe-DCNQI molecules[7,8] or by the selective deuteration among the eight protons in the DMe-DCNQI molecule. In particular, the latter affords a method to control the system without inhomogeniety inevitable in the alloying.[6] Besides, the alloy systems of the metallic $(DMe\text{-}DCNQI)_2Cu$ and the insulating Cu salt such as $(MeBr\text{-}DCNQI)_2Cu$ are demonstrated to span the critical region of the metal-insulator transition.[9]

Most interesting among the phenomena in this family of π-d electronic systems is the mechanism of the metal-insulator transition. The insulating phase is characterized by formation of the threefold superstructure and appearance of the charge ordering in the Cu sites, which gives a Curie-Weiss type of susceptibility.[3] The metal-insulator transition is proposed to result from cooperation between the Peierls transition in the quasi-one-dimensional π bands and the Mott transition in the strongly hybridized π-d bands with half-filling nature due to the superstructure formation,[10] which explains the extremely discontinuous transition with a large hysteresis. Several theoretical treatments show the roles of electron-phonon interaction, electron correlation, and dimensionality in the metal-insulator transition.[11,12]

On the other hand, interest had been directed to the metal-insulator boundary in expectation of the electronic states where the itinerant electrons interact with the localized Cu^{2+} spins such as the heavy electron systems. The resistivity of $(DMe\text{-}DCNQI)_2Cu$ under pressure[4,5] and the alloy systems, $[(DMe\text{-}DCNQI)_{1-x}(MeBr\text{-}DCNQI)_x]_2Cu$ and $[(DMe\text{-}DCNQI)_{1-x}(DBr\text{-}DCNQI)_x]_2Cu$ (Ref. 3), was studied with attention to the quadrature temperature dependence and the coefficient was discussed in the light of correlation

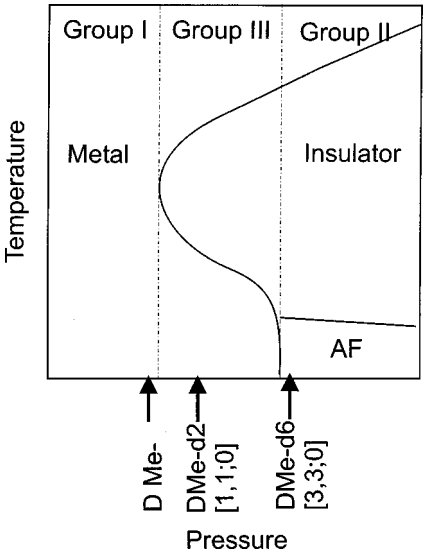

FIG. 1. Conceptual phase diagram of $(DCNQI)_2Cu$ systems. The vertical axis represents the effective (or chemical) pressure. AF denotes the antiferromagnetically ordered phase.

with the electronic specific heat coefficient, which was reported to be enhanced near the metal-insulator transition in the alloy systems.[3] As mentioned above, the partially deuterated systems of $(DMe\text{-}DCNQI)_2Cu$ also have access to the metallic region near the insulating transition with inhomogeneity minimized; interestingly, the residual resistance ratio of the reentrant metallic state of the partially deuterated system is larger than that of the nondeuterated system.[6] Although the susceptibility of the reentrant metallic phase was reported to be enhanced over the nondeuterated metallic value,[13] the subsequent measurements performed after a time enough to relax the supercooled state showed that there is no susceptibility difference between them.[14] The specific-heat study of this system is desirable, but unfortunately an excess entropy associated with symmetry breaking of the methyl group due to the partial deuteration gives a low-temperature giant peak of specific heat,[15] which overwhelms the electronic contribution.

The NMR serves as a microscopic characterization of the electronic states through the Knight shift and the line shape, which probe the static magnetic properties, and the spin-lattice relaxation rate, T_1^{-1}, which reflects the dynamic spin susceptibility. If electron mass or spin fluctuations are enhanced in the metallic phase near the insulator transition or in the reentrant metallic state, they can be detected through the NMR measurements.

The macroscopic quantities such as specific heat and magnetic susceptibility reflect the total contribution from the sample volume and therefore are not capable of characterizing each phase if several phases coexist in the sample, which may be the case in the vicinity of the metal insulator transition. Because of the spectroscopic feature of NMR, it can identify and examine each electronic phase separately.

Moreover, NMR is a site-sensitive probe. To date, the NMR measurements at the Cu (Refs. 16 and 17) and H (Ref. 18) sites were made for the present system. However, the behavior of T_1^{-1} is different in these two sites. In order to clarify the electronic state of the DMe-DCNQI site in more detail and the π-d interaction between DMe-DCNQI molecules and Cu atoms, the NMR measurement at each site of $=$N-CN in the DMe-DCNQI molecule is desired. However, the natural abundance of the $^{13}C(I=1/2)$ isotope is too small and NMR signals from other carbon sites complicate resultant spectra. Therefore, as the first step of our research, we replaced the carbon site of $=$N-CN in the DMe-DCNQI molecule to the ^{13}C isotope and measured the ^{13}C spin-lattice relaxation rate and Knight shift for a series of partially and nondeuterized $(DMe\text{-}DCNQI)_2Cu$ salts in order to examine the metallic state, the insulating state, and the transition between them.

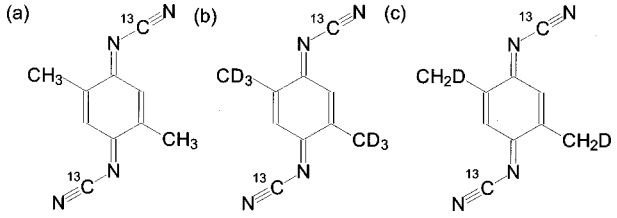

FIG. 2. DMe-DCNQI molecules with and without partial deuteration; (a) DMe-DCNQI-$h8$, (b) DMe-DCNQI-$d6[3,3;0]$ and (c) DMe-DCNQI-$d2[1,1;0]$. The ^{13}C substitution of the cyano carbon is for NMR measurements.

II. EXPERIMENT

We prepared three kinds of nondeuterated and partially deuterated DMe-DCNQI molecules with the ^{13}C isotope in the cyano (CN) group as shown in Fig. 2; (a) DMe-DCNQI-$h8$, which has no deuterium, (b) DMe-DCNQI-$d6[3,3;0]$, where all of the hydrogen in the methyl groups are replaced by deuterium, and (c) DMe-DCNQI-$d2[1,1;0]$, where only one hydrogen in each methyl group is replaced by deuterium. These notations follow Ref. 6.

These DMe-DCNQI molecules were synthesized from partially and nondeuterated p-phenylene-diamine using the isotope-labeled $K^{13}CN$.[1] The Cu salts were prepared by the chemical oxidation method. In order to characterize the magnetism and check paramagnetic impurities, static susceptibility was measured. As shown in Fig. 3, our sample of $(DMe\text{-}DCNQI\text{-}h8)_2Cu$ showed Pauli-like susceptibility in the whole temperature range,[19] $(DMe\text{-}DCNQI\text{-}d2[1,1;0])_2Cu$ showed a reentrant transition typical of group II and $(DMe\text{-}DCNQI\text{-}d6[3,3;0])_2Cu$ showed a transition from Pauli-like to Curie-Weiss behavior, followed by an antiferromagnetic transition at 7 K. The present results reproduce the previous ones in the literature so that these specimens can be situated in the generic phase diagram as shown in Fig. 1.

The ^{13}C NMR measurements were performed for powdered samples at an applied field of 8 T. The NMR spectra were obtained by the fast Fourier transformation (FFT) of the echo signal in the metallic state. In the insulating state, where the spectra are split into two sets of lines with a separation of the order of MHz, all of the spectra were constructed by measuring the echo intensity as a function of frequency at a fixed field. The relaxation rate was measured by the saturation recovery method.

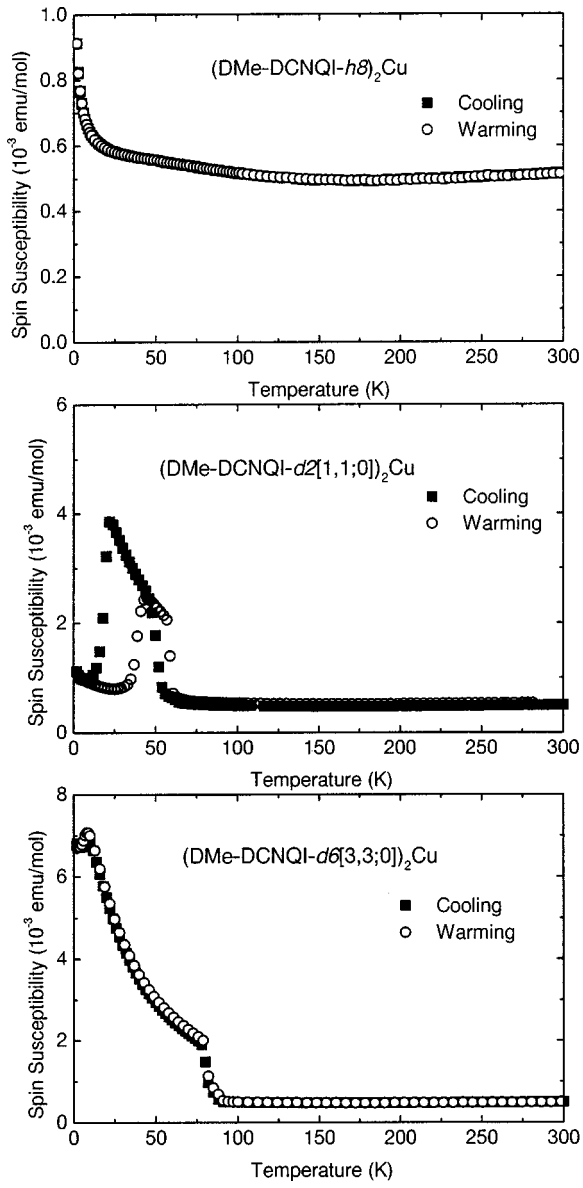

FIG. 3. Magnetic susceptibility of (DMe-DCNQI-$h8$)$_2$Cu, (DMe-DCNQI-$d2$[1,1;0])$_2$Cu, and (DMe-DCNQI-$d6$[3,3;0])$_2$Cu. The core-diamagnetic contribution is corrected.

III. RESULTS AND DISCUSSION

A. (DMe-DCNQI-$h8$)$_2$Cu (Group I)

In order to determine the absolute values of Knight shift of the (DMe-DCNQI)$_2$Cu systems, we used (DMe-DCNQI)$_2$Li as the reference system that gives the origin of the shift. The Li salt, where Li is monovalent and diamagnetic, has no π-d interaction in spite of the same crystal structure as (DMe-DCNQI)$_2$Cu and therefore the spin susceptibility originates from LUMO (lowest unoccupied molecular orbital) of DMe-DCNQI. This is in contrast with the case of (DMe-DCNQI)$_2$Cu, where the susceptibility comes from the DMe-DCNQI π electrons and the Cu d electrons. The Li salt is known to undergo the (spin) Peierls transition at 60 K, well below which the paramagnetic susceptibility vanishes. Therefore, the resonance frequency of this low-temperature state serves as the origin of the ^{13}C Knight shift for the (DMe-DCNQI)$_2$Cu systems. The low-temperature

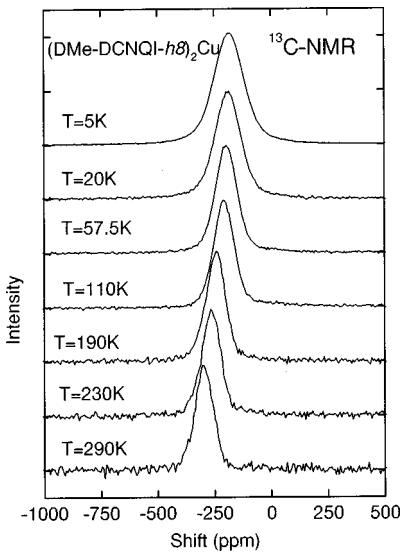

FIG. 4. ^{13}C NMR spectra of (DMe-DCNQI-$h8$)$_2$Cu.

spectra showed a powder pattern of the chemical shift tensor with uniaxial symmetry, of which the anisotropic terms are characterized by principal values of 70, 70, and -140 ppm. As the origin of the shift, we defined the center of gravity of the spectrum, namely, the first moment. Thus the determined value of the Knight shift of (DMe-DCNQI-$h8$)$_2$Cu is, for example, at room temperature, -300 ppm, which is in agreement with the previous report.[20]

From the orbital point of view, the hyperfine field at the ^{13}C site is generated by the electron spins on LUMO and d_{xy} orbitals. The LUMO contribution is further divided into two contributions. One is a hyperfine field from the spin on the on-site (carbon) $2p_z$ orbital, which exclusively participates in LUMO on the carbon site, if any. There, the core-polarization gives the isotropic term and the dipole field gives the anisotropic term. The other is from the spins on the neighboring nitrogen sites, which give isotropic and anisotropic fields at the ^{13}C site via the through-bond polarization and the dipole field, respectively. On the other hand, the d_{xy} contribution to the hyperfine field at the ^{13}C site is mainly an isotropic field via the through-bond polarization with the anisotropic dipole term playing a secondary role, being far from the carbon sites. The observed shift results from all these contributions.

Turning our attention to the experimental results in Fig. 4, one can observe symmetrical line shapes, which seemingly indicate the isotropic nature of the shift tensor in the metallic state. Considering that the chemical shift has the nearly uniaxial symmetry as mentioned above, the observed symmetry in the Cu salt should be due to the cancellation of the asymmetry in the chemical and spin shifts. Thus, the spin shift tensor at ^{13}C site is approximated as

$$\mathbf{T}=\begin{pmatrix} a-B & 0 & 0 \\ 0 & a-B & 0 \\ 0 & 0 & a+2B \end{pmatrix}, \qquad (1)$$

with $B\sim 70$ ppm. At room temperature, the isotropic a term is 300 ppm, which overwhelms the B term. According to the first-principles band calculation,[21] the carbon site is a node of LUMO of DCNQI, which means little participation of the

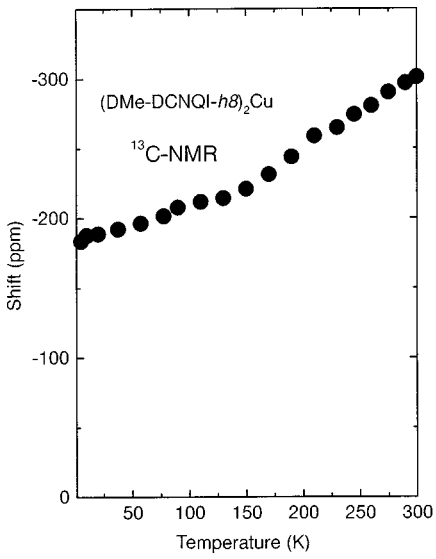

FIG. 5. Temperature dependence of ^{13}C isotropic Knight shift of (DMe-DCNQI-$h8$)$_2$Cu.

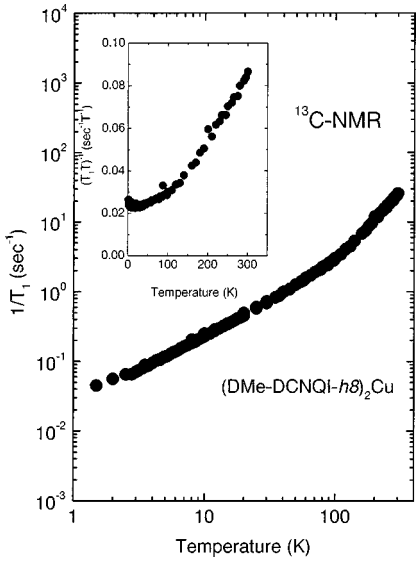

FIG. 6. Temperature dependence of ^{13}C nuclear spin-lattice relaxation rate of (DMe-DCNQI-$h8$)$_2$Cu. Inset shows temperature dependence of $(T_1T)^{-1}$.

carbon $2p_z$ orbital to LUMO. This explains why the anisotropic term, which is otherwise dominant due to the $2p_z$ dipole, is quite small. (In the case of the BEDT-TTF compounds, the anisotropic term is comparable to the isotropic one.[22]) In what follows, we discuss the isotropic shift K, which is expressed as

$$K = a^d \chi^d + a^{\mathrm{LUMO}} \chi^{\mathrm{LUMO}}. \tag{2}$$

Here, a^{LUMO} and a^d are the isotropic hyperfine coupling constants defined by the fields generated by one spin on LUMO and one spin on d_{xy} orbital, respectively, and χ^{LUMO} and χ^d are local spin susceptibility on each orbital. The experimentally observed total spin susceptibility, $\chi^{\mathrm{total}} = \chi^{\mathrm{LUMO}} + \chi^d$, is temperature insensitive as seen in Fig. 3(a). On the other hand, as shown in Fig. 5, the absolute value of K shows a monotonous decrease from 300 ppm at room temperature to 170 ppm at the low-temperature limit. The difference between the χ^{total} and K behaviors indicates a significant difference in the temperature dependence of the local spin susceptibility on the two sites as well as in the magnitude of a^{LUMO} and a^d. This fact is evidence that the present material is a multiband system since any single-band system should have the same temperature dependence in local susceptibility at any site.

The unit cell contains four DCNQI molecules and two Cu ions, of which the d_{xy} level is below the Fermi level, resulting in four Fermi surfaces with LUMO nature. According to the band structure calculations, two of the four are appreciably hybridized with the d_{xy} orbital. As the spin fluctuations are incoherent between the bands in the multiband system, K is rearranged as

$$K = \sum_{i=1}^{2} (a^{\mathrm{LUMO}} \chi_i^{\mathrm{LUMO}} + a^d \chi_i^d) + \sum_{i=3}^{4} a^{\mathrm{LUMO}} \chi_i^{\mathrm{LUMO}}, \tag{3}$$

where the index i denotes the band ($i=1$ and 2 specify the hybridized bands), and χ_i^{LUMO} and χ_i^d are the ith band components of the local spin susceptibilities, χ^{LUMO} and χ^d; namely, $\chi^{\mathrm{LUMO}} = \Sigma_{i=1}^4 \chi_i^{\mathrm{LUMO}}$ and $\chi^d = \Sigma_{i=1}^2 \chi_i^d$. Equation (3) is reformed into

$$K = \sum_{i=1}^{2} (a^{\mathrm{LUMO}} \rho_i^{\mathrm{LUMO}} + a^d \rho_i^d) \chi_i + \sum_{i=3}^{4} a^{\mathrm{LUMO}} \chi_i, \tag{4}$$

where χ_i is the spin susceptibility of the ith band, and ρ_i^{LUMO} and ρ_i^d are fractions of electron on each constituent orbital in the ith hybridized band. Then, the nuclear spin-lattice relaxation rate is expressed as

$$\frac{1}{T_1 T} = \frac{2 k_B \gamma_I^2}{\gamma_e^2 \hbar^2} \left[\sum_{i=1}^{2} (a^{\mathrm{LUMO}} \rho_i^{\mathrm{LUMO}} + a^d \rho_i^d)^2 \times \sum_{\mathbf{q}} \frac{\chi_i''(\mathbf{q}, \omega_N)}{\omega_N} + \sum_{i=3}^{4} (a^{\mathrm{LUMO}})^2 \sum_{q} \frac{\chi_i''(\mathbf{q}, \omega_N)}{\omega_N} \right]. \tag{5}$$

As seen in Eqs. (4) and (5), the hyperfine field from each band is additive in the Knight shift, while its square is additive in the spin-lattice relaxation rate. Therefore, comparison of the observed shift and relaxation rate is not straightforward in such a multiband system. However, we can get some insight into the relaxation rate in each band, taking into consideration the Cu-NMR results by Ishida *et al.*,[16] who observed that $(T_1T)^{-1}$ at the Cu site is insensitive to temperature with a slight enhancement above 100 K. The Cu site probes the spin fluctuations in the $i=1$ and 2 bands, namely, the first two terms in Eq. (5) although the hyperfine coupling constant is different from the above. These two bands have a three-dimensional nature due to the hybridization. In contrast, the present results of $(T_1T)^{-1}$ at the carbon site, which is given in Eq. (5), show a remarkably positive temperature dependence, as seen in Fig. 6; from $(T_1T)^{-1} = 0.023\ \mathrm{s}^{-1}\mathrm{K}^{-1}$ at low temperatures to $0.09\ \mathrm{s}^{-1}\mathrm{K}^{-1}$ at room temperature. Since the terms of $i=1$ and 2 should have

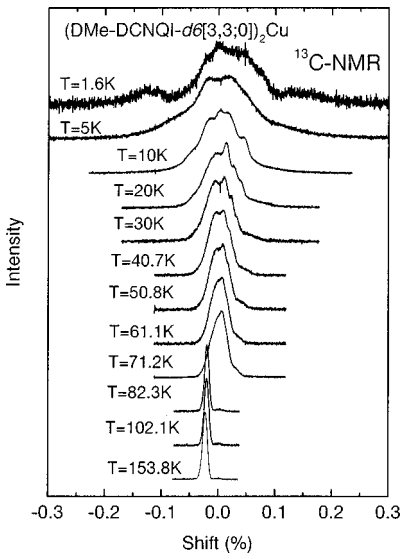

FIG. 7. ^{13}C NMR spectra of (DMe-DCNQI-$d6[3,3;0]$)$_2$Cu. Below 80 K, an additional line with a large shift beyond this scale (line 2), as shown in Fig. 9, appears.

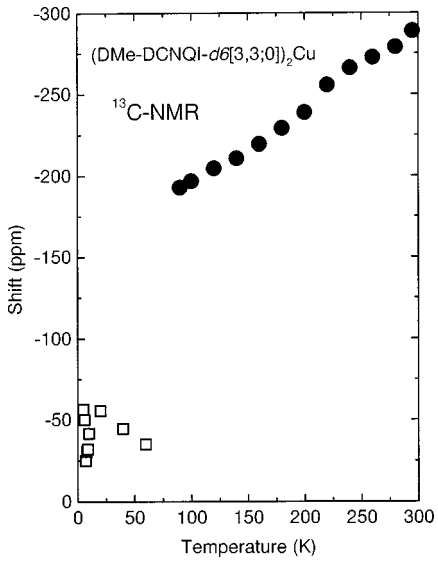

FIG. 8. Temperature dependence of ^{13}C isotropic Knight shift of (DMe-DCNQI-$d6[3,3;0]$)$_2$Cu. ● represents data in the metallic phase and □ represents data of line 1 (see text) in the insulating phase.

such a temperature dependence as in the Cu NMR, this peculiarity is attributable to the two terms of $i=3$ and 4; namely, the contributions from the nonhybridized one-dimensional LUMO bands.

Such a positive temperature-dependence of $(T_1T)^{-1}$ is also seen in the quasi-one-dimensional metallic systems of $(TMTSF)_2ClO_4$ and pressurized $(TMTSF)_2PF_6$ above 30 K, where TMTSF stands for tetramethyltetraselenafulvalene. Below this temperature, however, these salts show a remarkable enhancement in $(T_1T)^{-1}$ due to antiferromagnetic spin fluctuations because the systems are situated near the spin-density-wave (SDW) phase.[23] The absence of such a precursor in the present system is indicative of the qualitative difference between the present system and the TMTSF systems.

B. (DMe-DCNQI-$d6[3,3;0]$)$_2$Cu (group II)

Figures 7 and 8 show ^{13}C NMR spectra and Knight shift of (DMe-DCNQI-$d6[3,3;0]$)$_2$Cu. Above 80 K, where the metal-insulator transition occurs, the line shape and shift are nearly identical to those of (DMe-DCNQI-$h8$)$_2$Cu, showing that the metallic phases of the two salts are indistinguishable in nature. Below 80 K, the spectrum is changed into a broader line (denoted by line 1) around the 0 ppm position, which implies the decrease or vanishing of local spin susceptibility, giving the isotropic shift while the broadness reflects an increase in the anisotropic dipole field. The insulating phase is known to carry localized spins with the Curie-Weiss susceptibility, which is considered to be the origin of the dipole field. Curiously, the NMR signal intensity below 80 K is two-thirds of that in the metallic state above 80 K. Therefore, we searched for the missing NMR signal in a wider range of frequency and found it (denoted by line 2) with a large positive shift of the order of percent in the insulating phase, as shown in Fig. 9. It is noted that the sign of the shift is opposite to that of the metallic phase, suggesting that the hyperfine field at this carbon site in the insulating phase has a different origin from that of the metallic phase. The temperature dependence of the shift shown in Fig. 10 is characterized by the Curie-Weiss law with a Weiss temperature of -15.6 K, which is just the behavior of the spin susceptibility. The intensity ratio of line 1 to line 2 is about 2:1. In what follows, we discuss the origins of lines 1 and 2 appearing in the insulating state.

In the insulating state, the threefold superstructure with $c'=3c$ appears[24] and at the same time the charge separation into Cu^+ and Cu^{2+} with a population ratio of 2:1 is considered to occur.[3] The ^{1}H-NMR spectral profiles of a single-crystal (DMe-DCNQI-$d_7[3,3;1]$)$_2$Cu in the magnetically ordered state were consistent with the c-axis spin arrangement of $Cu^+Cu^+Cu^{2+}Cu^+Cu^+Cu^{2+}$ (Ref. 25). Moreover, the consideration of the compatibility of the threefold valence period with the crystal structure leads to the nearly unique

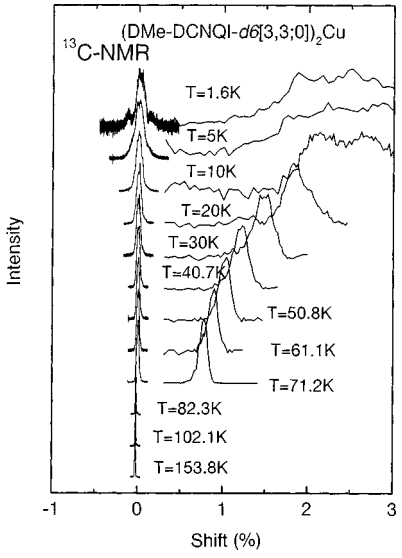

FIG. 9. ^{13}C NMR spectra of (DMe-DCNQI-$d6[3,3;0]$)$_2$Cu in a wide range of shift. A line with a large shift (line 2) appears in the insulating phase below 80 K. For convenience, the vertical axis for line 2 is expanded.

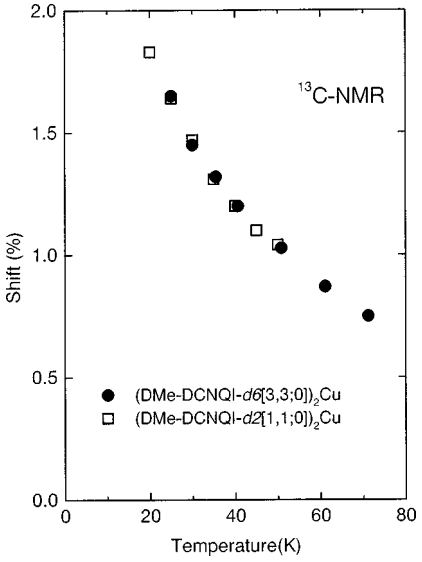

FIG. 10. Temperature dependence of ^{13}C isotropic Knight shift of line 2. ● for (DMe-DCNQI-$d6$[3,3;0])$_2$Cu and □ for (DMe-DCNQI-$d2$[1,1;0])$_2$Cu.

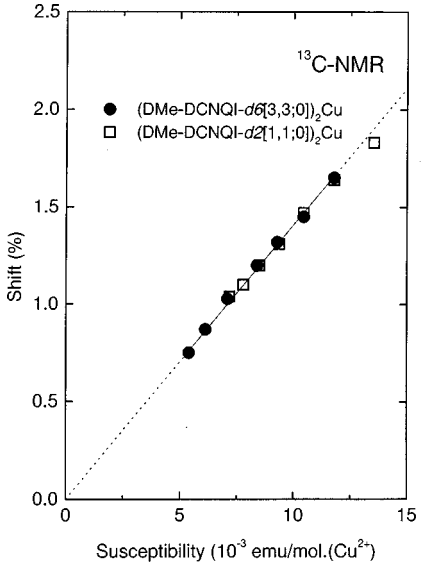

FIG. 12. The K-χ plot for line 2 (see text). ● for (DMe-DCNQI-$d6$[3,3;0])$_2$Cu and □ for (DMe-DCNQI-$d2$[1,1;0])$_2$Cu.

determination of the interchain charge arrangement as shown in Fig. 11 (Ref. 3). Since the structural analysis of the superstructure is not available, the crystallographical symmetry cannot be determined perfectly. From the magnetic point of view, however, there are expected to appear two kinds of DMe-DCNQI molecules, I and II, with a 1:2 population as shown in Fig. 11, where molecule II is coordinated by one Cu^{2+} and one Cu^{+}, while molecule I is coordinated by two Cu^{+}. Consequently, the carbon sites are divided into three

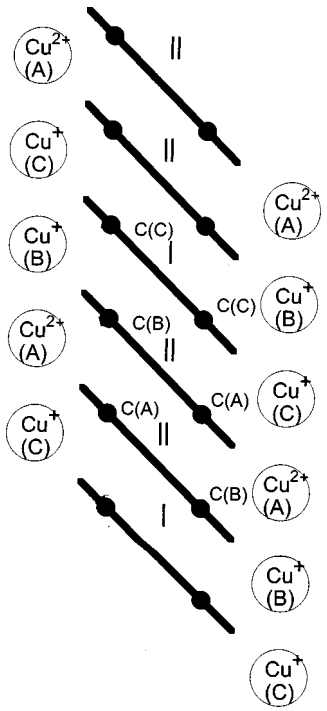

FIG. 11. A model of the Cu charge ordering in the insulating phase of (DMe-DCNQI)$_2$Cu, proposed in Ref. 3. The DCNQI-I is coordinated by two $Cu^{+}(C)$ and DCNQI-II is coordinated by $Cu^{+}(B)$ and $Cu^{2+}(A)$. The C(A), C(B), and C(C) stand for inequivalent ^{13}C sites due to the Cu charge ordering.

nonequivalent sites and the Cu sites also into the three sites; C(A) and C(B) in molecule II are located near $Cu^{2+}(A)$ and $Cu^{+}(B)$, respectively, and two C(C)'s on molecule I coordinated to $Cu^{+}(C)$ are equivalent. In this situation, we can make two possible site assignments of lines 1 and 2; one is that line 1 is from C(C) on molecule I and line 2 is from C(A) and C(B) on molecule II, while the other is that line 1 is from C(B) and C(C) coordinated to nonmagnetic Cu^{+} and line 2 is from C(A) coordinated to Cu^{2+}. The former picture is based on the assumption that the finite spin density is extended from $Cu^{2+}(A)$ into molecule II, which gives a large hyperfine field of line 2, while, in the latter picture, the Cu^{2+} spin makes the isotropic hyperfine field at the C(A) site by the through-bond polarization. In the former picture, the intensities of lines 1 and 2 should be in a ratio of 1:2 and the sign of the shift of line 2 is expected to be negative as in the metallic phase. The experimental intensity ratio of 2:1 and the positive shift observed are obviously against this picture but are consistent with the latter assignment, which gives the intensity ratio of 2:1. Therefore, it is concluded that the large local field giving line 2 comes from the through-bond core polarization along the pathway of C≡N-Cu due to the strong covalent bond of C≡N and that there is no spin fraction on DCNQI molecules because both of the C(B) and C(C) turned out to give line 1 with vanishing shift. Moreover, the latter fact confirms that the Cu(B) and Cu(C) sites coordinated to the cyano group with C(B) and C(C) carries no spin. These are microscopic evidence that the spin is localized exclusively at one-third of the Cu sites in the insulating phase. At the lowest temperature, the broadening of the spectra becomes prominent, as seen in Figs. 7 and 9. This is a manifestation of freezing of the dipole field due to the antiferromagnetic spin ordering.

Figure 12 shows a plot of the shift versus spin susceptibility (so-called K-χ) for line II. Here, χ is redefined per mole of Cu^{2+}. The relation is well fitted to a straight line with a slope of 1.4 mol (Cu^{2+})/emu, from which one gets the through-bond hyperfine coupling constant between the Cu^{2+} spin and ^{13}C nucleus as $a^d = 8.0$ kOe/μ_B(Cu^{2+}).

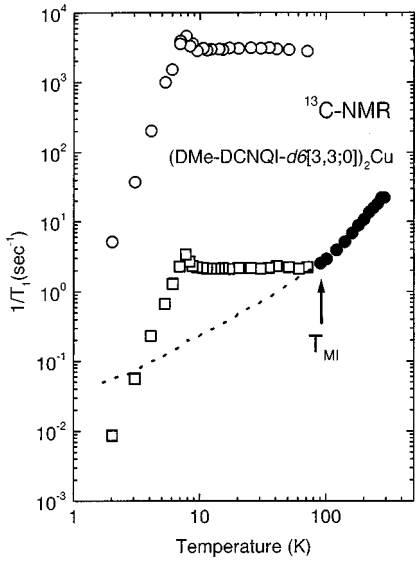

FIG. 13. Temperature dependence of ^{13}C nuclear spin-lattice relaxation rate of (DMe-DCNQI-d6[3,3;0])$_2$Cu. (● for the metallic phase, □ for line 1 and ○ for line 2 in the insulating phase) The dotted line represents the data of the metallic phase shown in Fig. 6.

The mixed valency or charge transfer, δ, in $Cu^{1+\delta}$ comes from the mixing of the d_{xy} orbital to the LUMO orbital at the Fermi level. Therefore, the hybridized band may well have spin density in the DCNQI molecule as well as in the Cu sites even after the disappearance of the nonhybridized one-dimensional Fermi surfaces due to Peierls instability. The present observation of absence of electron spins on the DCNQI molecules in the insulating phase clearly shows the localization of spins in one-third of the Cu sites exclusively. This spin location is not trivial in the above context but demonstrates that the threefold superstructure gives serious modifications in the band structure through splitting of the d_{xy} level due to the modulation of the tetrahedral coordination angle ($\angle$N-Cu-N) and that the electron correlation effect is enhanced by narrowing and possibly half-filling of the hybridized band after the Peierls transition. Such a decoupling between the d orbital and LUMO due to the correlation effect is postulated in the theoretical treatment.[26]

As shown in Fig. 13, the spin-lattice relaxation rate T_1^{-1} in the metallic phase above 80 K is also identical to that of (DMe-DCNQI-h8)$_2$Cu. These results again indicate no appreciable difference between the metallic states of the two systems. In the insulating phase below 80 K, the relaxation rate was measured in lines 1 and 2 separately. The magnitude of T_1^{-1} is different by three orders of magnitude between the two lines, reflecting the difference in the amplitude of local field fluctuations. However, their temperature dependence is nearly the same, which means that the two lines share the same source of the local field; namely, the Cu^{2+} spin. The T_1^{-1} keeps constant down to 10 from 80 K, as expected in a system of localized spins well above the Néel temperature. In the case of the powdered samples,[22] T_1^{-1} is expressed as[27]

$$T_1^{-1}=\frac{\sqrt{2\pi}g^2\gamma_n^2[(a^d)^2+2(B^d)^2]S(S+1)}{3\omega_{\rm ex}}, \qquad (6)$$

where

$$\omega_{\rm ex}^2=\frac{8zJ^2S(S+1)}{3\hbar^2} \quad \text{and} \quad T_N=\frac{|J|zS(S+1)}{3k_B}.$$

Here g is the averaged g value of the Cu^{2+} spins[28] ($\sim$2.19), γ_N is the gyromagnetic ratio of the ^{13}C nuclei, J is the exchange interaction energy between the spins of S, and z is the coordination number. The z is 4 in the present case where the interaction between Cu^{2+} is via the tetrahedrally coordinated DMe-DCNQI molecules by the superexchange mechanism. The direct exchange between Cu^{2+} spins is negligible since there is no overlap between the neighboring d orbitals. The J is evaluated from the Néel temperature of $T_N=8$ K. (The three dimensionality of the present spin network justifies the J evaluation from T_N.) The a^d and B^d are isotropic and anisotropic parts of the hyperfine coupling constant between ^{13}C site and Cu^{2+} spin.

For the C(B) and C(C) sites, a^d is nearly zero, as discussed above, and the B^d term is dominant. Calculation of dipole field from the nearest neighbor Cu^{2+} ion gives the values of $B^d=180$ Oe/$\mu_B(Cu^{2+})$ for C(B) and $B^d=44$ Oe/$\mu_B(Cu^{2+})$ for C(C), which has an appreciable second-neighbor contribution of $B^d=28$ Oe/$\mu_B(Cu^{2+})$. Using these values, T_1^{-1} is evaluated at 2.84 sec^{-1} for C(B) and 0.25 sec^{-1} for C(C). Since the measured relaxation rate of line 1 corresponds to an average of the two values because of the T_2 coupling of the two sites, the value to be compared with the experiment is 1.55 sec^{-1}, which gives a reasonable explanation to the observed value of 2.0 sec^{-1}. For the C(A) site giving line 2, the calculation gives a value of $B=300$ Oe/$\mu_B(Cu^{2+})$ while the isotropic term is $a^d=8.0$ kOe/$\mu_B(Cu^{2+})$, which is dominant for C(A). The evaluation with Eq. (6) yields $T_1^{-1}=2950$ sec^{-1}, of which the agreement with the experimental value of 2900 sec^{-1} is fairly good.

The Cu^{2+} dipole field at the C(A) site [$B^d=300$ Oe/$\mu_B(Cu^{2+})$] corresponds to a spectral width given by $\sim B^d\chi/N$, where the susceptibility χ is defined per molar Cu^{2+} and N is the Avogadro number. For example, at 40 K at the present field of 80 kOe, the width is evaluated at 0.05%, which is too small to reproduce the observed width of about 0.3% in full width at half maximum. On the other hand, the anisotropy of the spin susceptibility is $\Delta\chi/\bar{\chi}\approx 0.25$ (Ref. 14), which is also seen through the anisotropy in the g value.[28] This anisotropy should give a width in shift of 0.3% as the isotropic shift at 40 K is 1.2%. This explains the observed magnitude of the linewidth.

It is noted that there is observed no critical enhancement of T_1^{-1} near the M-I transition around 80 K. This clearly shows that the change of the spin dynamics is discontinuous and therefore the metal-insulator transition is of the first order. Below 10 K, T_1^{-1} exhibits a small enhancement and forms a sharp peak at 8 K, below which T_1^{-1} shows a steep decrease. This behavior is typical of the antiferromagnetic ordering.

C. (DMe-DCNQI-d2[1,1;0])$_2$Cu (group III)

The (DMe-DCNQI-d2[1,1;0])$_2$Cu with one deuterium in each methyl group of DCNQI shows a reentrant (metal-insulator-metal) transition. The NMR measurements were

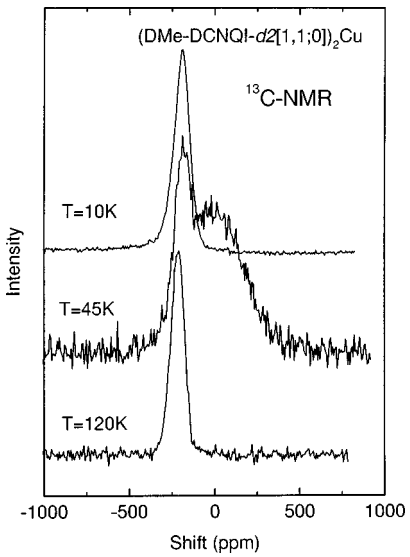

FIG. 14. ^{13}C NMR spectra of (DMe-DCNQI-$d2[1,1;0]$)$_2$Cu. In the insulating phase between 17 and 50 K, an additional line with a large shift (line 2), which is not shown here, appears.

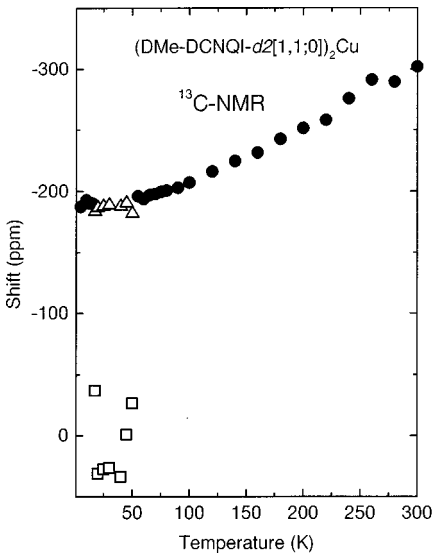

FIG. 15. Temperature dependence of ^{13}C isotropic Knight shift of (DMe-DCNQI-$d2[1,1;0]$)$_2$Cu. (● are for the single line in the metallic phase, and □ and △ are for the two lines observed in the intermediate temperature range, as shown in Fig. 14).

made at descending temperatures. Figure 14 shows the NMR spectra of (DMe-DCNQI-$d2[1,1;0]$)$_2$Cu at several temperatures. Above the M-I transition ($\sim$50 K), the line shape is nearly identical to those observed in the metallic states of the previous two systems. In the intermediate temperature range between 17 and 50 K, where the system is postulated to be insulating, a broad line with the same character as in the insulating state of the (DMe-DCNQI-$d6[3,3;0]$)$_2$Cu appears with a smaller fraction of the metal-phase signal remaining. The coexistence of metallic and insulating phases in the intermediate temperature region was seen in ^{63}Cu-NMR as well.[17] This is due to supercooling of part of the sample or to inhomogeneous internal pressure. Below 17 K, the broader line suddenly merges into the narrower line, indicating that the metallic phase is stabilized in the whole volume. As shown in Fig. 15, the isotropic Knight shift of the metallic phases of the (DMe-DCNQI-$d2[1,1;0]$)$_2$Cu is identical to the previous ones. In the temperature range between 17 and 50 K, we observed an additional NMR signal with a large positive shift as in the case of the (DMe-DCNQI-$d6[3,3;0]$)$_2$Cu salt. The position of the signal, which is plotted as a function of temperature in Fig. 10 and as a function of spin susceptibility in Fig. 12, follows the behavior of the (DMe-DCNQI-$d6[3,3;0]$)$_2$Cu salt exactly.

The T_1^{-1} is plotted in Fig. 16. The high-temperature ($>$50 K) and low-temperature ($<$17 K) metallic phases show quantitatively similar behavior to the metallic (DMe-DCNQI-$h8$)$_2$Cu. The relaxation rate of the insulating phase appearing in the intermediate temperatures traces those of the insulating phase of the (DMe-DCNQI-$d6[3,3;0]$)$_2$Cu salt. These results of the shift and relaxation rate of the (DMe-DCNQI-$d2[1,1;0]$)$_2$Cu salt clearly indicate that the metallic and insulating states have no critical behavior even in the vicinity of the metal-insulator transition and that this transition is of the first order.

IV. CONCLUDING REMARKS

In the present study, we have investigated the metallic and insulating states and the transition between them in (DMe-DCNQI)$_2$Cu with different degrees of deuteration by ^{13}C-NMR at the cyano-site of the DMe-DCNQI molecule. By comparison of the total spin susceptibility and ^{13}C Knight shift in the metallic phase, this system is shown to have several electronic bands with different temperature dependence of spin susceptibility. In the insulating phase, the electron spins are found to be localized at one-third of the Cu sites exclusively without appreciable population at the DCNQI sites, while they are distributed over the DCNQI sites and Cu sites in the metallic phase. This fact, which is difficult to understand in the band picture of the π-d hybrid-

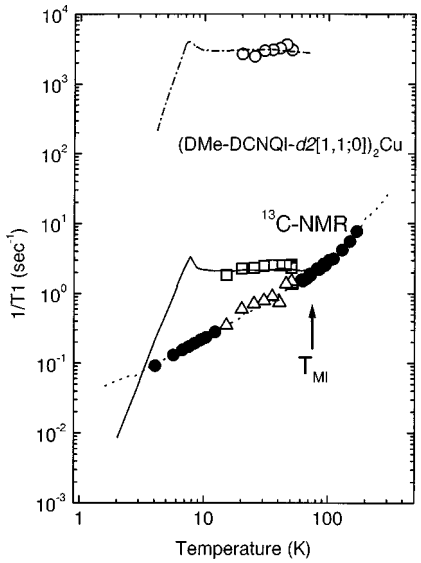

FIG. 16. Temperature dependence of ^{13}C nuclear spin-lattice relaxation rate of (DMe-DCNQI-$d2[1,1;0]$)$_2$Cu. (● are for the metallic phase, △ are for metallic component, ○ and □ are for line 1 and line 2 observed in the insulating phase, respectively.) The dash-dotted and solid lines represent the data of (DMe-DCNQI-$d6[3,3:0]$)$_2$Cu and the solid line represents the data of (DMe-DCNQI-$h8$)$_2$Cu.

ization, is a manifestation of the electron correlation in this family of materials.

The present ^{13}C-NMR study also shows that the metal-insulator transition is discontinuous. The metallic and insulating phases have no critical fluctuations in the shift and relaxation rate even in the vicinity of the transition. The reentrant metallic phase is found to have the same character as the metallic phase far from the metal-insulator boundary. These findings provide microscopic evidence that the metal-insulator transition is of the first order.

ACKNOWLEDGMENTS

The authors thank Professor R. Kato and Dr. S. Aonuma for their useful suggestions on synthesis of the DMe-DCNQI-$d2[1,1;0]$ molecules and preparation of the Cu salts. They are also grateful to Professor Yonemitsu and Dr. Ogawa for their stimulating discussion on the theoretical aspect. This work was supported in part by Grant-in-Aid for Scientific Research No. 09440145 and Grant-in-Aid for COE Research.

[1] A. Aumüller, P. Erk, G. Klebe, S. Hünig, J. U. von Schütz, and H. P. Werner, Angew. Chem. Int. Ed. Engl. **25**, 740 (1986).
[2] R. Kato, H. Kobayashi, and A. Kobayashi, J. Am. Chem. Soc. **111**, 5224 (1989).
[3] H. Kobayashi, A. Miyamoto, R. Kato, F. Sasaki, A. Kobayashi, Y. Yamakita, Y. Furukawa, M. Tasumi, and T. Watanabe, Phys. Rev. B **47**, 3500 (1993).
[4] T. Mori, K. Imaeda, R. Kato, A. Kobayashi, H. Kobayashi, and H. Inokuchi, J. Phys. Soc. Jpn. **56**, 3429 (1987).
[5] S. Tomic, D. Jérome, A. Aumüller, P. Erk, S. Hünig, and J. U. von Schütz, J. Phys. C **21**, L203 (1988).
[6] S. Aonuma, H. Sawa, R. Kato, and H. Kobayashi, Chem. Lett. **1993**, 513.
[7] R. Kato, H. Sawa, S. Aonuma, M. Tamura, M. Konoshita, and H. Kobayashi, Solid State Commun. **85**, 831 (1993).
[8] D. Bauer, J. U. von Schütz, H. C. Wolf, S. Hünig, K. Sinzger, and R. K. Kremer, Adv. Mater. **5**, 229 (1993).
[9] Y. Nishio, K. Kajita, W. Sasaki, R. Kato, A. Kobayashi, and H. Kobayashi, Solid State Commun. **81**, 473 (1992).
[10] H. Fukuyama, in *Correlation Effects in Low-dimensional Electron Systems*, edited by A. Okiji and N. Kawakami (Springer-Verlag, Berlin, 1994), p. 128.
[11] T. Ogawa and Y. Suzumura, J. Phys. Soc. Jpn. **63**, 2066 (1994).
[12] K. Yonemitsu, Phys. Rev. B **56**, 7262 (1997).
[13] H. Sawa, M. Tamura, S. Aonuma, R. Kato, M. Kinoshita, and H. Kobayashi, J. Phys. Soc. Jpn. **62**, 2224 (1993).
[14] M. Tamura, H. Sawa, S. Aonuma, R. Kato, and M. Kinoshita, J. Phys. Soc. Jpn. **63**, 429 (1994).
[15] Y. Noshio, N. Someya, T. Tega, H. Kobayashi, K. Kajita, S. Aonuma, H. Sawa, and R. Kato, Synth. Met. **71**, 1947 (1995).
[16] U. Langohr, J. U. von Schütz, H. C. Wolf, H. Meixner, and S. Hünig, Synth. Met. **41-43**, 1855 (1991).
[17] K. Ishida, Y. Kitaoka, H. Masuda, K. Asayama, T. Takahashi, A. Kobayashi, R. Kato, and H. Kobayashi, J. Phys. Soc. Jpn. **64**, 2970 (1995).
[18] K. Kanoda, T. Tamura, T. Ohyama, T. Takahashi, R. Kato, H. Kobayashi, and A. Kobayashi, Synth. Met. **42**, 1843 (1991); T. Takahashi, K. Kanoda, T. Tamura, K. Hiraki, K. Ikeda, R. Kato, H. Kobayashi, and A. Kobayashi, Synth. Met. **55-57**, 2281 (1993).
[19] R. Kato *et al.* [Synth. Met. **70**, 1071 (1995)] reported that the ^{13}C substitution at the cyano groups in (DMe-DCNQI-$h8)_2$Cu shifts the effective pressure by ca. 100 bars, which leads the system to the Group II, in contrast to the present result.
[20] H. Helmle, J. Reiner, U. Rempel, M. Mehring, J. U. von Schütz, P. Erk, H. Meixner, and S. Hünig, Synth. Met. **41-43**, 1763 (1991).
[21] T. Miyazaki and K. Terakura, Phys. Rev. B **54**, 10 452 (1996).
[22] A. Kawamoto, K. Miyagawa, Y. Nakazawa, and K. Kanoda, Phys. Rev. B **52**, 15 522 (1995).
[23] D. Jérome, in *Organic Conductors*, edited by Jean-Pierre Farges (Marcel Dekker, New York, 1994), p. 405.
[24] A. Kobayashi, R. Kato, H. Kobayashi, T. Mori, and H. Inokuchi, Solid State Commun. **64**, 45 (1987).
[25] K. Hiraki, Y. Kobayashi, T. Nakamura, T. Takahashi, S. Aonuma, H. Sawa, R. Kato, and H. Kobayashi, J. Phys. Soc. Jpn. **64**, 2203 (1995).
[26] T. Ogawa and Y. Suzumura, Phys. Rev. B **53**, 7085 (1996); T. Ogawa and Y. Suzumura, J. Phys. Soc. Jpn. **66**, 690 (1997).
[27] T. Moriya, Prog. Theor. Phys. **16**, 23 (1956); **16**, 641 (1956).
[28] T. Mori, H. Inokuchi, A. Kobayashi, R. Kato, and H. Kobayashi, Phys. Rev. B **38**, 5913 (1988).